



HAL
open science

Short term precursors of Strombolian explosions at Yasur volcano (Vanuatu)

Jean Battaglia, Jean-Philippe Métaxian, Esline Garaebiti

► **To cite this version:**

Jean Battaglia, Jean-Philippe Métaxian, Esline Garaebiti. Short term precursors of Strombolian explosions at Yasur volcano (Vanuatu). *Geophysical Research Letters*, 2016, 43 (5), pp.1960 - 1965. 10.1002/2016GL067823 . hal-01636977

HAL Id: hal-01636977

<https://uca.hal.science/hal-01636977v1>

Submitted on 20 May 2021

HAL is a multi-disciplinary open access archive for the deposit and dissemination of scientific research documents, whether they are published or not. The documents may come from teaching and research institutions in France or abroad, or from public or private research centers.

L'archive ouverte pluridisciplinaire **HAL**, est destinée au dépôt et à la diffusion de documents scientifiques de niveau recherche, publiés ou non, émanant des établissements d'enseignement et de recherche français ou étrangers, des laboratoires publics ou privés.



RESEARCH LETTER

10.1002/2016GL067823

Key Points:

- Repeating LPs related to processes deeper than explosion quakes at a Strombolian volcano
- LPs are commonly followed by explosions with a variable precursory delay
- We propose a causal relationship linked to pressure transfer

Correspondence to:

J. Battaglia,
J.Battaglia@opgc.univ-bpclermont.fr

Citation:

Battaglia, J., J.-P. Métaxian, and E. Garaebiti (2016), Short term precursors of Strombolian explosions at Yasur volcano (Vanuatu), *Geophys. Res. Lett.*, *43*, 1960–1965, doi:10.1002/2016GL067823.

Received 15 JAN 2016

Accepted 18 FEB 2016

Accepted article online 20 FEB 2016

Published online 12 MAR 2016

Short term precursors of Strombolian explosions at Yasur volcano (Vanuatu)

Jean Battaglia¹, Jean-Philippe Métaxian², and Esline Garaebiti³

¹Laboratoire Magmas et Volcans, Université Blaise Pascal—CNRS-IRD, OPGC, Aubière, France, ²ISTerre, IRD R216, CNRS, Université de Savoie, Le Bourget du Lac, France, ³Vanuatu Meteorology and Geohazards Department, Port Vila, Vanuatu

Abstract The seismic wavefield associated with Strombolian activity is usually dominated by explosion quakes (EQs), tremor, and various signals generated by surface phenomena. Looking at the seismicity recorded at Yasur volcano in 2008, we found that beside the transient events which occur simultaneously with surface explosions, the seismicity includes events related to a deeper process. These long period (LP) events form a family of similar events located below the southeastern part of the crater rim at a depth of about 700–1200 m below the summit. They are commonly followed by EQs with a variable delay. The examination of about 20,000 LP-EQ sequences at several stations near the summit shows that interevent delays follow distributions peaked around 11–12 s. This short delay compared to the relatively great source depth of the LPs favors a causal relationship linked to pressure transfer rather than gas slug propagation after nucleation at the LP source.

1. Introduction

Strombolian activity at volcanoes is characterized by the repetition of low amplitude explosions emitting ash and block and more or less continuous gas emissions. This type of activity is frequently observed at volcanoes, sometimes quasi-permanently like at Stromboli (Italy) or Yasur and sometimes more occasionally like at Tungurahua (Ecuador) or Etna (Italy) for example. Diverse seismic signals are generally associated to Strombolian activity, especially at a close distance (several kilometers) from the vents. In the short period frequency range, explosion quakes (EQs), with frequencies mainly between 1 and 5 Hz, are observed directly associated to the explosions [Ripepe, 1996]. They frequently include a high frequency (>5 Hz) acoustic air wave [Braun and Ripepe, 1993; Ripepe and Braun, 1994] and are commonly located between the surface and a few hundred meters below. They are often directly associated to the bursting of gas slugs at the free surface of the conduit. More or less permanent tremor is frequently observed [Wassermann, 1997; Chouet et al., 1997] associated with continuous degassing. At frequencies below 0.5 Hz, very long period (VLP) signals are observed [Neuberg et al., 1994; Rowe et al., 1998; Chouet et al., 2003] often simultaneously with explosions. They are typically attributed to the coalescence [Ripepe et al., 2001] or ascent [James et al., 2006; Chouet et al., 2008] of gas slugs.

Yasur volcano is a small scoria cone (360 m asl) located on Tanna island, in the southern part of Vanuatu. It is characterized by permanent Strombolian explosive activity, with up to several explosions per minute. These explosions are issued from three vents named A, B, and C (Figure 1) located in the summit crater. This crater is subdivided in two subcraters with vents A and B sharing the same southern subcrater. Associated with its activity, seismic instruments record up to 2000 short period transient signals per day as shown below, as well as long duration tremor and VLP signals.

In this paper, we examine in the short period frequency range (>0.5 Hz) the seismicity recorded in 2008 at Yasur volcano in order to identify characteristic similar events. This characterization outlines the presence of a category of events related to a deeper process and we examine the relationship between these events and EQs.

2. Data and Characteristic Seismic Events

From January 2008 to February 2009 we operated around Yasur volcano a temporary seismic network which included up to 22 stations: 10 Guralp CMG-40 T broadband sensors and 12 seismic antennas, each equipped with up to nine short period sensors with a 2 Hz corner frequency (Figure 1). Short period stations were installed at the end of January 2008 and broadband stations at the mid-May. All stations were removed at the beginning of February 2009. The stations continuously recorded the activity on local harddrives which

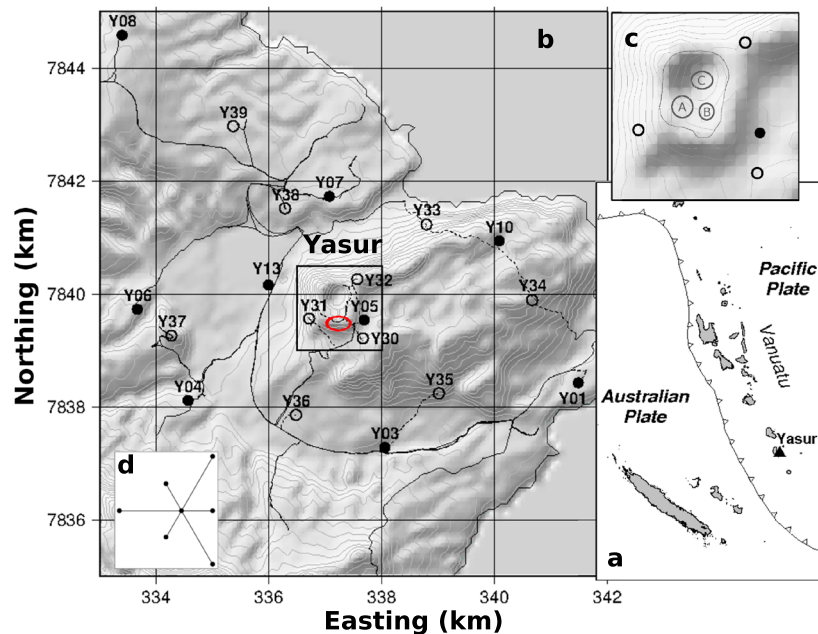


Figure 1. Geological settings and layout of the seismic network. (a) Location of Yasur volcano in Vanuatu archipelago. (b) Location of the seismic stations from the temporary deployment. Short period seismic antennas are indicated by black filled circles and broadband stations are indicated by empty circles. Map is in UTM kilometric coordinates. Contour lines are plotted every 25 m elevation. The approximate epicentral location of LP events is indicated by a red ellipse. (c) Summit area of Yasur volcano corresponding to the black rectangle shown in Figure 1b. Approximate location of the crater rim is indicated by a dotted line as well as the rough location of the three active vents. (d) Typical sensor distribution for a seismic antenna: one three-component sensor surrounded by six vertical sensors at distances of 20 or 40 m.

were collected on a regular basis. To correlate seismic recording with field observations we also acquired several hours of video recordings which have been synchronized precisely with GPS time.

To extract meaningful information from the hundreds of transient signals recorded per day and simplify their analysis, we attempted to identify the characteristic events as detailed by Battaglia *et al.* [2015]. For this purpose, we searched for families of repeating signals at a station (Y05) which is one of the closest to the summit crater (400 m); it was also installed since the beginning of the experiment in January 2008 and displays simple waveforms as compared to other summit stations. We first applied an STA/LTA algorithm with an LTA (long time average) of 60 s, a STA (short time average) of 1 s, and a minimum time lag between two successive events of 8 s. To consider a maximum number of transients, we used a low threshold and extracted signal windows for each event with an STA/LTA higher than 2.5. These signal windows have been compared to each other using cross correlation to determine families of similar events. We use a similarity threshold of 0.8 to group events. Because of the large number of events with a total of 371,940 detections during our study period, the procedure was done on a daily basis and for each family a daily stack was generated by summing the similar waveforms after aligning them. Finally, all stacks have been compared to each others to determine reference events for the different families.

The result of the classification outlines the presence of at least 40 families corresponding to stacks with distinct waveforms [Battaglia *et al.*, 2015]. Several families dominate the activity with a few of them lasting for several months or the entire duration of the experiment. Most of these families group EQs as attested by the presence of clear high frequency acoustic phases and/or according to correlations with video recordings and field observations. However, we also note the presence of two families of events which are not synchronous with explosions. At all stations, most of their energy is found between 1 and 3 Hz. They are related to deeper processes and we interpret them as corresponding to long period (LP) events commonly observed on volcanoes [Chouet, 1996]. The two families only differ because of minor distortions in the coda induced by the occurrence of a $M=7.3$ subduction earthquake [Battaglia *et al.*, 2012] on 9 April 2008 (day 100 in Figure 2). We hereafter consider them as a single family.

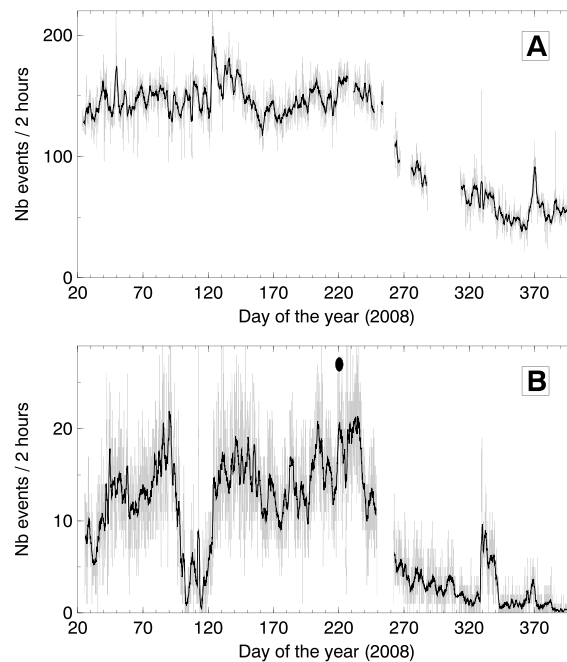


Figure 2. (a) Number of events per 2 h detected at station Y05 with a STA/LTA higher than 2.5. (b) Temporal evolution of the number of LP events detected at station Y07 using matched filtering with a reference stacked waveform whose origin time is indicated by a black filled ellipse. On both plots, number of events is shown in gray color with a thick black line showing an average over 20-point windows.

These stacks have been used to pick the onsets of about 6000 events. Using a simplified 1-D velocity model and a version of hypo71 [Lee and Lahr, 1975] adapted to take into account the station elevation, we found LP source locations at about 700–900 m bsl and below the southern rim of the crater. Finally, Battaglia *et al.* [2015] showed that amplitude ratios between stations Y05 and Y07 suggest that LP sources are significantly deeper than those for most of the EQ families.

3. Precursory LP Events

To recompute the temporal evolution of the number of LPs during our experiment, we use station Y07 located 2 km from the summit instead of Y05 as it is less dominated by shallow EQ activity and therefore displays more clearly deeper LP waveforms. We identify LPs by cross-correlation a reference LP stack with the continuous data (matched filtering). This reference event was generated by summing LP waveforms from Y07, recorded on a same day chosen during a period of high activity, and identified based on the catalog of LP events at Y05. Using this technique, we identify up to 39,000 LPs with a correlation higher than 0.7 with the reference stack over the 374 days of the experiment. The events occurred with an average rate of about 5–7 events per hour during the 7.5 first months and their number decreased toward the end of the experiment, following roughly the temporal evolution of the total number of detected transients which are mostly related to the volcanic activity (Figure 2a). A drop in the number of LPs identified by matched filtering is observed between 6 April (97) and 2 May (123) because of the waveform change induced by the occurrence of a $M = 7.3$ subduction earthquake on 9 April 2008 (100) 80 km from the volcano [Battaglia *et al.*, 2012]. Similar procedure applied to several other stations around the summit identifies less events because of more complex waveforms but provides comparable temporal evolutions to the one in Figure 2b.

Aligning similar LPs at Y05 on their precisely known and common onset times, which were determined by matched filtering, shows that most of them are followed by EQs with a variable delay (Figure 3). To precisely determine interevent delays, we examined thousands of LP-EQ sequences recorded at the four stations located at the summit (Y05, Y30, Y31, and Y32) and at Y07. For this purpose we used two techniques to estimate the time difference between the onset of the LP (known from LP detection) and the onset of the first

Preliminary locations for LPs were obtained with two independent methods. Perrier [2011] used an array technique to locate LPs and EQs based on the calculation of time delays between each pair of seismometers to estimate the slowness vector and thus the direction of the source from each seismic antenna. The epicentral position was determined by intersecting these directions. The source depth of EQs was estimated by using the mean time delay measured between the P wave and the acoustic wave for events where the onsets of these waves were clearly observable. The estimation of the depth for LPs is based on the difference of apparent velocity, estimated with the slowness vector calculation, between LPs and EQs. Perrier [2011] found LP sources at about 400–800 m bsl and a few hundred meters west-south-west of the summit (red ellipse in Figure 1b). Sources for EQs were found mostly at shallow depths in the first 400 m below the summit. As an alternate solution to locate LPs, we built stacked waveforms for all stations in order to improve the identification of first arrival

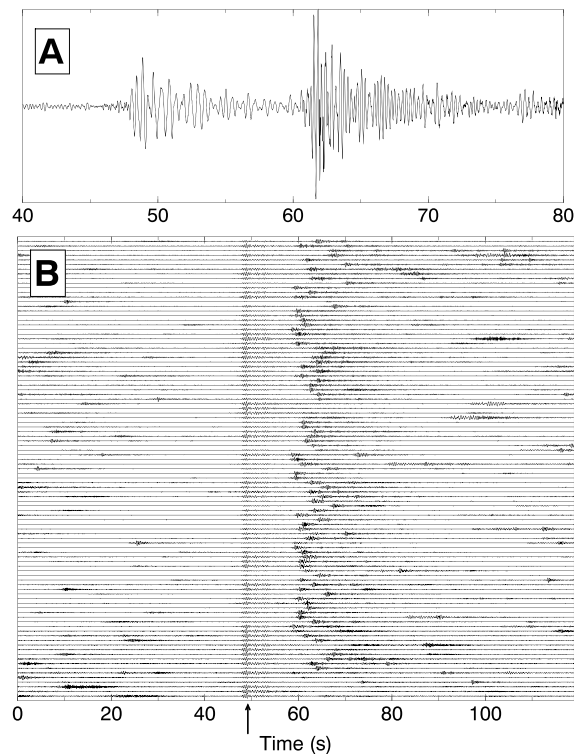


Figure 3. (a) Typical 40 seconds sequence recorded at one of the vertical components of station Y05 showing an LP followed by an explosion quake. (b) Plot showing 100 sequences similar to the one shown in Figure 3a. Similar LP events are aligned near second 50 as indicated by the black arrow at the bottom of the plot. On most traces, the LP events are followed by explosion quakes occurring with a variable delay.

sequences identified at station Y05 and 39000 at station Y07. Both techniques indicate delays following comparable distributions which are peaked between 11 and 12 s. Histograms obtained using STA/LTA include short interevent delays below 5 s mostly because of secondary triggering in the late part of the LPs themselves. The highest precision is obtained with matched filtering at station Y05 because of clearer EQ waveforms near the vent. The asymmetrical distribution shows interevent delays mainly above 9 s and is peaked between 11 and 12 s. The presence at Y07 of shorter delays with matched filtering is mostly due to misidentifications as EQs have

following EQ. First, an STA/LTA detection technique was used to identify the onset of the first following EQ. The technique allows the processing of all LP-EQ sequences but unfortunately only provides an approximate estimation of the EQ onsets because of emergent waveforms. Also, for this same reason, an empirical correction between 1 and 4 s, depending on the station and its distance to the summit, was applied because of systematically overestimated delays with this technique (Figure 4). This correction was estimated for each station from the offset between the two histograms (obtained by STA/LTA and matched filtering as explained hereafter) and confirmed by visual inspection of the position of the pickings on the waveforms. Second, we used matched filtering and reference stacks for the identified families of EQs. Each of the LP-EQ sequences has been scanned with all available EQ reference stacks [Battaglia *et al.*, 2015] to identify possible similar waveforms following the LPs. This technique allows a precise identification of individual EQ onsets because of the improved determination of onsets on the more impulsive reference stacks. However, it does not allow the identification of all EQs in the sequences as only those similar to one of the reference events can be recognized.

Figure 4 presents histograms for delays obtained using both techniques applied to 20,000 LP-EQ

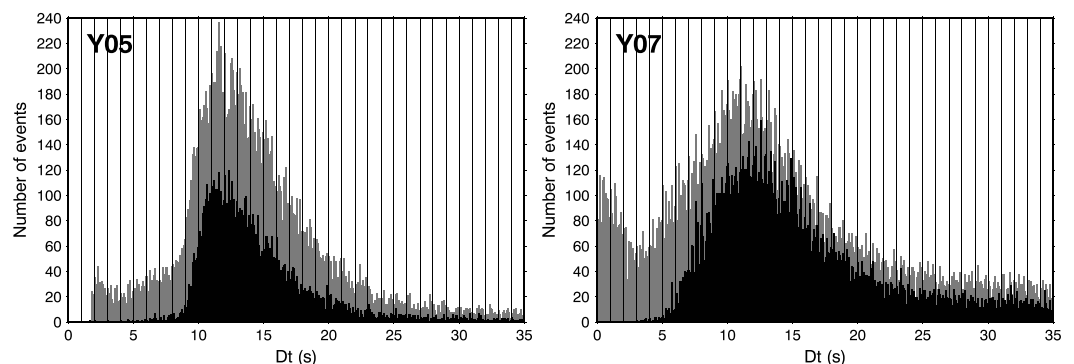


Figure 4. Histograms showing the number of delays per interval of 0.1 s for (left) 20,000 LP-EQ sequences recorded at station Y05 and (right) 39,000 sequences recorded at station Y07. The higher number of LP events identified at Y07 is explained by simpler waveforms and better signal to noise ratio at that station. Gray histograms show delays calculated using STA/LTA. Black histograms show delays precisely identified using matched filtering and reference traces for LP events and EQ.

often unclear and elongated waveforms at 2 km from the vent. Comparable distributions were also obtained at the other summit stations with, however, less success in the identification using matched filtering.

No clear temporal evolution of the interevent delay is observed during the experiment. Also no clear relation is observed between the amplitude of the LP and that of the following EQ. An important pattern is that LPs are not observed prior to every EQ and reversely some LPs are not followed by any clear EQ. This could be due to LPs and EQs being too small to be detected, as well as to different processes in explosion triggering. To estimate rough statistics, we note that for the period between the end of January and mid-October 2008 about 250,000 different EQs have been identified at Y05 by matched filtering using the 38 EQ reference stacks while for the same period about 36,000 LPs were identified at Y07 suggesting that no more than 15% of the EQs could be preceded by LPs. On the other hand we note that from the 19,725 LP-EQ sequences examined at Y05, 74% include an event detected by STA/LTA starting between 8 and 20 s after the onset of the LP, 64% between 8 and 17, and 52% between 8 and 15.

4. Discussion and Conclusions

Among the hundreds of daily transient signals, mostly EQs, related to the Strombolian activity of Yasur, we identified a family of similar LP events related to a deeper process. Most of these events are followed by EQs with a variable delay whose distribution is peaked between 11 and 12 s. The classification technique which we used on a large scale and the search for characteristic events allowed the identification of a unique causal relationship between two different types of events. Further work is needed to identify such sequences at other volcanoes. The short term precursory aspect of the LPs and its role in the generation of explosions remains, however, uncertain.

Commonly, Strombolian explosions are assumed to be caused by the outburst of gas slugs. In the frame of this model, a tentative explanation would be that LPs are directly related to the propagation of these slugs. Such events could occur at specific locations along the conduit such as places where a diameter change is observed [James *et al.*, 2006] or at the top of the magma reservoir where slug coalescence occurs [Jaupart and Vergnolle, 1988]. However, the relatively great depth of the LP source (700–1200 m below the summit) and relatively short delay between the onset of the LPs and following EQs whose sources are mostly between 300 and 90 m below the summit [Perrier, 2011] would require a slug propagation ascent rate of about 40–90 m/s. These values are in the range of velocities calculated at Stromboli by Harris and Ripepe [2007] and Gurioli *et al.* [2014] based on seismic, infrasonic, and thermal observations. However, these authors conclude that their values are an order of magnitude higher than those calculated for a conduit with a diameter of several meters [Seyfried and Freundt, 2000] based on fluid dynamics and analog experiments. The modeling of the rapid near-surface expansion of gas slugs provides elevated velocities only for the propagation of its nose [James *et al.*, 2008].

Alternately, we propose that LP events may occur independently of the slug propagation, being caused by any pressure fluctuation related to unsteady mass transport [Chouet, 1996]. They could be the source of a pressure wave which would propagate upward along the conduit. Such a wave would travel at a higher velocity ranging from a several hundred meters per second if we assume a crack wave [Ferrazzini and Aki, 1987] or several kilometers per second if we assume P wave velocity and pressure propagation through the solid matrix [Chouet *et al.*, 2008]. Gas slug may coalesce independently at shallower depth and their upward propagation could be triggered by the pressure wave. This model could therefore also explain the absence of visible EQs after some of the LPs as the pressure wave will not trigger any slug propagation if the slug coalescence is not sufficiently advanced. Inversely, slug ascent may also occur without the passage of the pressure wave, explaining the absence of any visible LP prior to many explosions.

References

- Battaglia, J., J. P. Métaxian, and E. Garaebiti (2012), Earthquake-volcano interaction imaged by coda wave interferometry, *Geophys. Res. Lett.*, *39*, L11309, doi:10.1029/2012GL052003.s
- Battaglia, J., J. P. Métaxian, and E. Garaebiti (2015), Families of similar events and modes of oscillation of the conduit at Yasur volcano (Vanuatu), *J. Volcanol. Geotherm. Res.*, doi:10.1016/j.jvolgeores.2015.11.003.
- Braun, T., and M. Ripepe (1993), Interaction of seismic and air waves recorded at Stromboli Volcano, *Geophys. Res. Lett.*, *20*(1), 65–68, doi:10.1029/92GL02543.
- Chouet, B. (1996), Long-period volcano seismicity: Its source and use in eruption forecasting, *Nature*, *380*, 309–316.

Acknowledgments

All the data used in this study were collected during a temporary experiment carried with seismic stations from the French seismic networks IHR and RISC (Isterre, Grenoble, France). We are grateful to D. Nakedau, S. Byrdina, and R. Yatika who helped significantly in field work. We thank also two anonymous reviewers who helped to greatly improve the manuscript. This work has been supported by the ANR (France) contract ANR-06-CAT-02 Arc-Vanuatu. The data used for this publication are available upon request to the corresponding author.

- Chouet, B., G. Saccorotti, M. Martini, P. Dawson, G. De Luca, G. Milana, and R. Scarpa (1997), Source and path effects in the wave fields of tremor and explosions at Stromboli Volcano, Italy, *J. Geophys. Res.*, *102*(B7), 15,129–15,150, doi:10.1029/97JB00953.
- Chouet, B., P. Dawson, T. Ohminato, M. Martini, G. Saccorotti, F. Giudicepietro, G. De Luca, G. Milana, and R. Scarpa (2003), Source mechanisms of explosions at Stromboli Volcano, Italy, determined from moment-tensor inversions of very-long-period data, *J. Geophys. Res.*, *108*(B1), 2019, doi:10.1029/2002JB001919.
- Chouet, B., P. Dawson, and M. Martini (2008), *Shallow-Conduit Dynamics at Stromboli Volcano, Italy, Imaged From Waveform Inversions*, *Geol. Soc. London, Special Publ.*, *307*, 57–84.
- Ferrazzini, V., and K. Aki (1987), Slow waves trapped in a fluid-filled infinite crack: Implication for volcanic tremor, *J. Geophys. Res.*, *92*, 9215–9223, doi:10.1029/JB092iB09p09215.
- Gurioli, L., L. Colo, A. J. Bollasina, A. J. L. Harris, A. Whittington, and M. Ripepe (2014), Dynamics of Strombolian explosions: Inferences from field and laboratory studies of erupted bombs from Stromboli volcano, *J. Geophys. Res. Solid Earth*, *119*, 319–345, doi:10.1002/2013JB010355.
- Harris, A. J. L., and M. Ripepe (2007), Synergy of multiple geophysical approaches to unravel explosive eruption conduit and source dynamics—A case study from Stromboli, *Chem. Erde*, *67*, 1–35.
- James, M. R., S. J. Lane, and B. A. Chouet (2006), Gas slug ascent through changes in conduit diameter: Laboratory insights into a volcano-seismic source process in low-viscosity magmas, *J. Geophys. Res.*, *111*, B05201, doi:10.1029/2005JB003718.
- James, M. R., S. J. Lane, and S. B. Corder (2008), *Modelling the Rapid Near-Surface Expansion of Gas Slugs in Low-Viscosity Magmas*, *Geol. Soc. London, Spec. Publ.*, *307*, 147–167.
- Jaupart, C., and S. Vergnolle (1988), Laboratory models of Hawaiian and Strombolian eruptions, *Nature*, *331*, 58–60.
- Lee, W. H. K. and J. C. Lahr (1975), HYPO71 (revised): A computer program for determining hypocenter, magnitude, and first motion pattern of local earthquakes, *U.S. Geol. Surv. Open File Rep.*, *75-311*, US Geological Survey, Washington, D. C.
- Neuberg, J., R. Luckett, M. Ripepe, and T. Braun (1994), Highlights from a seismic broadband array on Stromboli volcano, *Geophys. Res. Lett.*, *21*(9), 749–752, doi:10.1029/94GL00377.
- Perrier, L. (2011), *Apport de l'étude des sources sismo-volcaniques à la connaissance des processus éruptifs du volcan Yasur, Vanuatu*, Phd thesis, Université de Grenoble, France.
- Ripepe, M. (1996), Evidence for gas influence on volcanic seismic signals recorded at Stromboli, *J. Volcanol. Geotherm. Res.*, *70*(3), 221–233.
- Ripepe, M., and T. Braun (1994), Air-wave phases in Strombolian explosion-quakes seismograms: A possible indicator for the magma level, *Acta Vulcanol.*, *5*, 201–206.
- Ripepe, M., S. Ciliberto, and M. Della Schiava (2001), Time constraints for modeling source dynamics of volcanic explosions at Stromboli, *J. Geophys. Res.*, *106*(B5), 8713–8727, doi:10.1029/2000JB900374.
- Rowe, C. A., R. C. Aster, P. R. Kyle, J. W. Schlue, and R. R. Dibble (1998), Broadband recording of Strombolian explosions and associated very-long-period seismic signals on Mount Erebus, Ross Island, Antarctica, *Geophys. Res. Lett.*, *25*, 2297–2300, doi:10.1029/98GL01622.
- Seyfried, R., and A. Freundt (2000), Experiments on conduit flow and eruption behavior of basaltic volcanic eruptions, *J. Geophys. Res.*, *105*, 23,727–23,740, doi:10.1029/2000JB900096.
- Wassermann, J. (1997), Locating the sources of volcanic explosions and volcanic tremor at Stromboli volcano (Italy) using beam-forming on diffraction hyperboloids, *Phys. Earth Planet. Inter.*, *104*(1), 271–281.